

See discussions, stats, and author profiles for this publication at: <https://www.researchgate.net/publication/236836346>

Solvent modulated photophysics of 9-methyl anthroate: Exploring the effect of polarity and hydrogen bonding on the emissive state

ARTICLE in SPECTROCHIMICA ACTA PART A MOLECULAR AND BIOMOLECULAR SPECTROSCOPY · APRIL 2013

Impact Factor: 2.35 · DOI: 10.1016/j.saa.2013.04.059 · Source: PubMed

CITATIONS

9

READS

39

5 AUTHORS, INCLUDING:



Aniruddha Ganguly

University of Calcutta

19 PUBLICATIONS 67 CITATIONS

[SEE PROFILE](#)

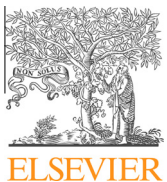


Sankar Jana

Tohoku University

33 PUBLICATIONS 351 CITATIONS

[SEE PROFILE](#)



Contents lists available at SciVerse ScienceDirect

Spectrochimica Acta Part A: Molecular and Biomolecular Spectroscopy

journal homepage: www.elsevier.com/locate/saa

Solvent modulated photophysics of 9-methyl anthroate: Exploring the effect of polarity and hydrogen bonding on the emissive state

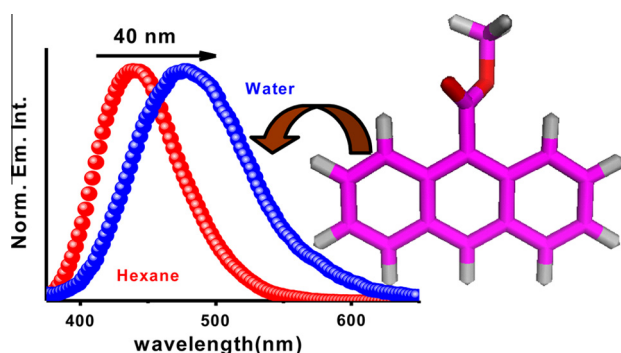
Aniruddha Ganguly, Sankar Jana, Soumen Ghosh, Sasanka Dalapati, Nikhil Guchhait*

Department of Chemistry, University of Calcutta, 92, A.P.C. Road, Kolkata 700 009, India

HIGHLIGHTS

- Solvatochromic behavior of 9-MA exploited by fluorimetry.
- Evidence of the emissive state to be the Franck–Condon state.
- Multiple linear regression analysis to quantify the effect of hydrogen bonding.
- Urea induced H-bonding disruption study.
- Theoretical calculations to support the experimental findings.

GRAPHICAL ABSTRACT



ARTICLE INFO

Article history:

Received 19 January 2013

Received in revised form 5 April 2013

Accepted 10 April 2013

Available online 22 April 2013

Keywords:

9-Methyl anthroate

Dipole moment

Multiple linear regression

Hydrogen bonding

Non-radiative decay constants

ABSTRACT

Photophysical properties of an anthracene derivative 9-methyl anthroate (9-MA) have been investigated using absorption and emission spectroscopy, in combination with quantum chemical calculations. Solvatochromic effects on the Stokes shifted emission band clearly demonstrate the highly polar character of the excited state, which is also supported by the enhancement of dipole moment of the molecule upon photoexcitation. The emission band has been found to be dependent on polarity and hydrogen-bonding ability of the solvents. Multiple linear regression analysis method has been utilized to rationalize the effect of hydrogen bonding interaction on the emissive state, which was further confirmed by the analysis of the non-radiative decay constants and urea induced H-bonding disruption study. The experimental results correlate well with theoretical predictions obtained via density functional theory (DFT).

© 2013 Elsevier B.V. All rights reserved.

Introduction

Anthracene based fluorophores stand out owing to their simple structure, facile synthetic procedure and high fluorescence quantum yields [1,2]. Generally, fused ring hydrocarbons are referred to as potential carcinogens, but surprisingly a recently reported anthracene based metabolite, Alterporriol L, isolated from a marine fungus, is found to show cytotoxicity against different types of cancer cells [3,4], whereas as obvious some derivatives are known to be uniquely mutagenic and cytotoxic in both bacterial and mam-

malian cells [5]. Anthracene derivatives are widely studied because of their enormous ability to sense biologically relevant ions, especially alkaline earth and transition metal ions, not only through specific binding but also via inhibition of photoelectron transfer [6–10]. Anthracene derivatives also have potential applications in the manufacturing of OLEDs and field-effect transistors which are frequently used in flat panel displays and smart cards [11,12], and are effective singlet oxygen producer from the first excited singlet and triplet states [13]. There are even reports of anthracene based fluorophores being used as membrane probes [14]. Photodimerization of anthracene derivatives, especially of esters has also been exhaustively studied, even in solid state [15,16]. It has been first noticed by Werner et al. that substitution on the anthracene

* Corresponding author. Tel.: +91 3323508386; fax: +91 3323519755.

E-mail address: nguchhait@yahoo.com (N. Guchhait).

nucleus has a marked influence on its photophysical properties [17], which was also confirmed by Schuster via ^{13}C NMR spectroscopy [18]. Werner and co workers have also investigated the fluorescence characteristics of 9-anthroic acid and some ester derivatives of it in mixed solvents (ethanol–water and dioxane–water) as well as in a few pure solvents, though the studies are not so detailed and lack any theoretical support [19,20]. Thus, explicit photophysical studies on such derivatives are still a requirement from scientific point of view.

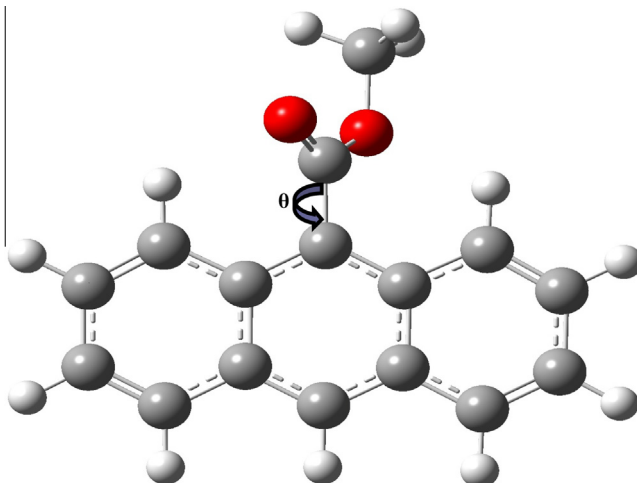
Solvation studies of fluorophores, especially those containing polar substituents on the aromatic ring/s draw considerable attention to researchers, owing to the influence of solvents on the corresponding fluorescence spectra and quantum yields, which may arise from the perturbations due to solvent refractive index and dielectric constant or from intermolecular hydrogen bonding between the fluorophore and the solvent or even from complexation between the fluorophore and the solvent [21,22]. These factors modulate the energy gap between the ground (S_0) and the first excited singlet (S_1) state and thus cause a shifting in the emission spectra and/or affect quantum yields. The polarity and the hydrogen bonding ability of the solvents are known to be the key factors in modulating the routes of energy dissipation from the electronic excited state, especially when the emissive state is polar [22–24]. Also, as proposed by Lim, solvent-moderated shifts of the energy levels may enhance or inhibit non-radiative transitions to the ground state [25].

Our present work aims towards a detailed photophysical study of 9 methyl anthroate (Scheme 1), which is known to inhibit Cl^- conductance across the epithelial membrane and fatty acid incorporation into phospholipids in human airway epithelial cells [26], in various pure solvents differing in polarity and hydrogen bonding ability by using absorption and emission spectroscopy. The target of the study is to explore the effect of polarity and hydrogen bonding on the radiative transitions of this compound from the excited singlet state explicitly. Finally, the results obtained from the experimental studies have been rationalized with quantum chemical calculations.

Materials and methods

Materials

9-Methyl anthroate (Scheme 1) was synthesized and purified according to the literature procedure [27]. For a detailed description of synthesis and purification, see Supporting Information.



Scheme 1. Ground state optimized structure of 9-MA obtained at DFT (B3LYP/6-311++G(d,p)) level.

Spectroscopic grade solvents such as *n*-hexane (HEX), cyclohexane (CY), carbon tetrachloride (CCl₄), dioxane (DOX), tetrahydrofuran (THF), chloroform (CHCl₃), dichloromethane (DCM), dimethylformamide (DMF), dimethyl sulfoxide (DMSO), acetonitrile (ACN), isopropanol (PrOH), *n*-butanol (BuOH), ethanol (EtOH) and methanol (MeOH) were purchased from Spectrochem, India and were used after proper distillation as required. Urea was procured from E-Merck, India and was recrystallized from methanol before use. Triple distilled water was used for preparing the aqueous solutions.

Instrumental details

The absorption and emission spectral measurements were done by Hitachi UV-vis U-3501 spectrophotometer and Perkin-Elmer LS-55 Luminescence spectrophotometer, respectively. In all measurements the sample concentration was maintained in the range of $\sim 10^{-6}$ M in order to avoid aggregation and reabsorption effects. All absorption and emission spectral measurements have been performed at room temperature with proper background corrections and with air-equilibrated, freshly prepared solutions only.

Fluorescence lifetimes were measured by the method of Time Correlated Single-Photon counting (TCSPC) using a HORIBA Jobin Yvon Fluorocube-01-NL fluorescence lifetime spectrometer. The sample was excited using a picosecond laser diode at 375 nm and the signals were collected at the magic angle of 54.7° to eliminate any considerable contribution from fluorescence anisotropy decay [21,28,29]. The typical time resolution of our experimental set-up is ~ 100 ps. The decays were deconvoluted using DAS-6 decay analysis software. The acceptability of the fits was judged by χ^2 criteria and visual inspection of the residuals of the fitted function to the data. Mean (average) fluorescence lifetimes were calculated using the following equation [28,29]:

$$\tau_{av} = \frac{\sum \alpha_i \tau_i^2}{\sum \alpha_i \tau_i}$$

in which α_i is the pre-exponential factor corresponding to the *i*th decay time constant, τ_i .

Fluorescence quantum yield (Φ_f) was determined using quinine sulfate as the secondary standard ($\Phi_f = 0.54$ in 0.1 M H₂SO₄) using the following equation [30,31],

$$\Phi_S = \Phi_R \frac{A_S}{A_R} \times \frac{(Abs)_R}{(Abs)_S} \times \frac{\eta_S^2}{\eta_R^2}$$

where "A" terms denote the integrated area under the fluorescence curve, "Abs" denote absorbance, η the refractive index of the medium and Φ , the fluorescence quantum yield. Subscripts "S" and "R" stand for denoting respective parameters for the studied sample and reference, respectively.

Computational details

All theoretical calculations except the excited-state optimization of the ester were performed in Gaussian 03W suite of programs [32] whereas the latter has been done in Gaussian 09W suite of programs [33]. The global minimum energy optimized structure of the ester in vacuo was obtained by optimizing the geometry at DFT (density functional theory) level using B3LYP hybrid functional (which comprises of Becke's three parameter hybrid exchange functional in conjunction with the nonlocal correlation functional of Lee, Yang and Parr). For this purpose 6-311++G(d,p) basis set has been chosen because this basis set is of triple- ζ quality for valence electrons with diffuse functions which are useful in calculations for anions and structures with lone pair electrons [34,35]. To get the optimized structure of the molecule in solvents of different polarity, the Polarizable Continuum model

(PCM) method was used applying the corresponding keywords implemented in the software. In this method, the solute, treated quantum chemically, is placed in a cavity surrounded by the solvent. The latter is considered as a continuum characterized by its bulk properties, such as dielectric constant or polarity [35]. Highest Occupied Molecular Orbital (HOMO) and Lowest Unoccupied Molecular Orbital (LUMO) diagrams were also constructed from the optimized structure.

Results and discussions

Absorption spectra

Absorption spectra of 9-MA recorded in various solvents show a structured band with a maximum near 360 nm (Fig. 1a). The spectral band maxima observed in different solvents are presented in Table 1. This broad absorption band is assigned to the $S_1 \leftarrow S_0$ transition of the anthracene chromophore [17,19]. High absorption intensity of the band is indicative of its being a $\pi-\pi^*$ type transition, which is also supported by the indifference of the absorption spectra towards the addition of protic acid. The absorption band exhibits slight dependence on solvent polarity. A slight red shift (~ 5 nm) of the absorption maxima with increasing solvent polarity is rationalized in anticipation with progressively greater degree of stabilization of the excited state in polar environments. This observation relates well with the signature of a polar excited state (π^* state is more polar and thus more stabilized in polar solvents resulting such red shift) and is consistent with literature reports [36–38]. A slight blue shift of the band position in methanol and water in comparison to less polar solvents DMSO might seem a little puzzling but is not unlikely owing to the possible intermolec-

ular hydrogen bonding interaction between the ester and these protic solvents [39]. This argument seems justified on the ground of efficient hydrogen bonding ability of methanol and water and is in harmony with several reports with aromatic molecules containing polar groups [37,39]. The minute red shift of the band position in water as compared to methanol may be attributed to greater polarity of water than methanol. Although it is the solvent polarity which is most often invoked to account for the medium polarity-dependent emissions, the role of specific properties of solvent such as hydrogen bonding ability, dielectric constant, etc. might be instrumental in some cases in governing the photophysics of such molecules [37]. The impact of such specific interactions in governing the overall photophysics of 9-MA has been clearly demonstrated through a detailed analysis of solvatochromic parameters in the forthcoming sections.

Emission and excitation spectra

The single emission band of the molecule recorded in various solvents by excitation at the respective absorption maxima are shown in Fig. 1b and the position of the emission band maxima are presented in Table 1. In *n*-hexane, a broad emission band is observed with a maximum at ~ 440 nm. The emission maximum is found to be gradually red-shifted with increasing polarity of the solvent. This solvatochromic red-shift of about 40 nm (from ~ 440 nm in *n*-hexane to ~ 480 nm in water) supports for the polar character of the emissive state. It is anticipated that greater stabilization of the polar photoexcited state in solvents of higher polarity produces the observed solvatochromic red-shift of the emission band. That there exists only a single species in the ground state and the observed phenomenon is exclusively an excited state

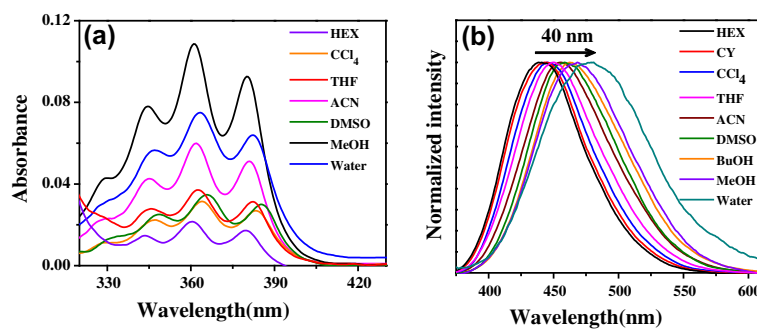


Fig. 1. (a) The room temperature absorption spectra of 9-methyl anthroate in different solvents as indicated in the figure legend. (b) Fluorescence emission spectra of 9-methyl anthroate in different solvents as indicated in the figure legend (exciting at the corresponding absorption band maxima).

Table 1

Spectroscopic parameters and quantum yield of 9-methyl anthroate in solvents of different polarity at room temperature.

Solvents	E_T (30)	λ_{max} (abs) in nm	λ_{max} (em) in nm	$\Delta\bar{v}(\text{cm}^{-1})$	Quantum yield (ϕ_f)
HEX	30.9	360	440	5050	0.201
CY	31.2	360	443	5204	0.193
CCl ₄	32.5	361	445	5000	0.251
DOX	36.0	363	452	5424	0.221
THF	37.4	363	450	5326	0.205
CHCl ₃	39.1	362	448	5638	0.122
DCM	41.1	364	455	5494	0.303
DMF	43.8	363	456	5618	0.121
DMSO	45.0	363	455	5583	0.133
ACN	46.0	362	455	5646	0.106
iPrOH	48.6	361	462	6056	0.058
BuOH	50.2	363	463	5950	0.075
EtOH	51.9	362	465	6119	0.043
MeOH	55.5	361	468	6333	0.021
H ₂ O	63.1	363	480	6043	0.010

process, is confirmed by a good juxtaposition of the fluorescence excitation spectra in various solvents assayed (Fig. S1 in the Supporting information) with the absorption spectra.

Polarity and H-bonding effect on the emissive state of 9-MA

To get a quantitative idea about the polarity of the emissive state, the dipole moment of the emissive state has been calculated using the method proposed by Lippert [23,36]. According to his proposition, the dipole moment of the emissive state can be calculated from the solvatochromism of the UV absorption and the fluorescence spectra using the following relations,

$$\bar{v}_a = \mu_g \frac{(\mu_{FC} - \mu_g)}{2\pi\epsilon_0 hc\rho^3} \Delta f(\epsilon_r, \eta) + \text{Const}$$

$$\bar{v}_f = \mu_{ss} \frac{(\mu_{ss} - \mu_g)}{2\pi\epsilon_0 hc\rho^3} \Delta f(\epsilon_r, \eta) + \text{Const}$$

$$\text{where } \Delta f(\epsilon_r, \eta) = \left[\frac{\epsilon_r - 1}{2\epsilon_r + 1} \right] - \left[\frac{\eta^2 - 1}{2\eta^2 + 1} \right]$$

In this equation, \bar{v}_a and \bar{v}_f are the positions of the absorption and emission band maxima in cm^{-1} , respectively, whereas Δf is the solvent polarity parameter. The symbols h , c , ρ , ϵ_0 and η represent Planck's constant, speed of light, Onsager cavity radius, permittivity of vacuum and refractive index of the medium, respectively. The terms μ_g , μ_{FC} and μ_{ss} are the dipole moments corresponding to the ground state, Franck–Condon excited state and solvent stabilized excited state of the system. Now, for the optimized global minimum structure of 9-MA (calculated at DFT level of theory using B3LYP hybrid functional and 6-311++G(d,p) basis set), the value of ' ρ ' and ' μ_g ' are found to be 5.15 Å and 1.77 D, respectively. From the slope of \bar{v}_a vs. Δf plot (Fig. S2a in the Supporting information), the dipole moment of the Franck–Condon state is calculated to be 3.32 D. Such an increase in dipole moment of the compound from the ground to the excited state further corroborates to the enhanced polarity of the emissive state and hence justifies the red-shift of the emission maxima with polar solvents through solvent stabilization. Interestingly, the dipole moment of the solvent stabilized excited state, calculated from the slope of \bar{v}_f vs. Δf plot (Fig. S2b in the Supporting information) is found to be 3.48 D which is almost same as that of the FC state, which strongly suggests that the Franck–Condon state is the emissive one and thereby wipes off the presence of any charge transfer phenomenon. However, for both the cases, the deviation from linearity in the plot for polar protic solvents (not shown in the figures) indicates that solute–solvent hydrogen-bonding interactions have a substantial effect on the emission band [40,41]. In this context it is worth to mention that the plot of the emission maxima (in cm^{-1}) against hydrogen-bonding parameter ' α ' is found to be linear (Fig. 2), which further substantiate the effect of solute–solvent hydrogen-bonding interactions and thus points towards the potential applicability of the aforesaid probe as a quantifier of the hydro-

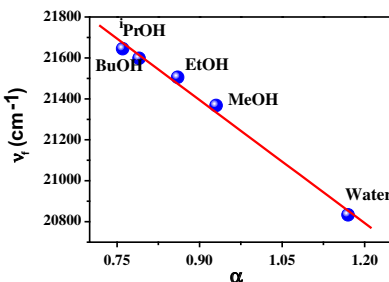


Fig. 2. Correlation of emission maxima (in cm^{-1}) of 9-methyl anthroate in different protic solvents with the H-bonding parameter α of the solvents.

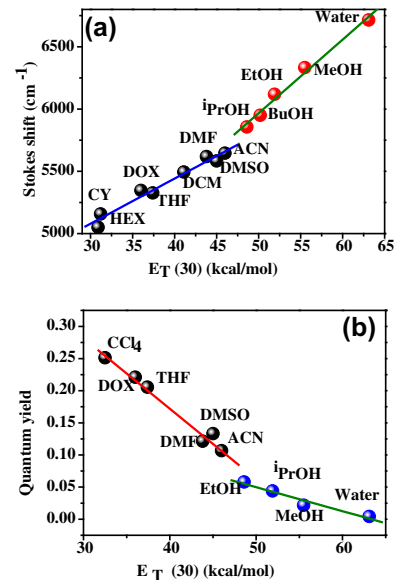


Fig. 3. (a) Plot of Stokes shift ($\Delta v/\text{cm}^{-1}$) vs. polarity parameter ($E_T(30)/\text{kcal mol}^{-1}$) for 9-methyl anthroate, as obtained from spectroscopic measurements in various solvents. (b) Plot of quantum yield of the compound against $E_T(30)$ parameter of the solvents.

gen bonding ability of a solvent. The correlation of Stokes shift (in cm^{-1}) with the solvent dependent $E_T(30)$ parameter [42] is shown in Fig. 3a where two distinct lines are observed, one for the non-hydrogen-bonding solvents (non-polar and polar aprotic) and the other for the polar protic solvents. This indicates that both electrostatic dipolar and hydrogen-bonding interactions influence the emission of the compound of interest.

Such H-bonding interaction might also open up non-radiative decay paths in protic solvents. This possibility is indeed reflected in the lowering of quantum yields observed in solvents of increasing hydrogen bonding characters. The measured fluorescence quantum yields of the compound are presented in Table 1. The quantum yield values show a remarkable decrease with increasing polarity of the solvents up to the polar aprotic limit and then in the solvents with H-bonding capability the rate of decrement drops. Such an observation may be attributed to differential contribution of electrostatic dipolar and hydrogen bonding interactions [43,44]. However, as mentioned before, increasing intermolecular hydrogen-bonding ability of the solvents makes way for the accessibility of some non-radiative decay channels which deplete the quantum yield of the ester (9-MA) by almost an order of magnitude than in the corresponding polar aprotic solvents. The significant lowering of quantum yield of the emission from acetonitrile to water is hence explained on the basis of the increasing hydrogen bonding strength of water. The plot of quantum yield against $E_T(30)$ parameter of the solvents (Fig. 3b), also reflects the fact where two distinct lines with different slopes are observed.

In order to get acumen into the different modes of solvation determining the absorption and fluorescence energies, the multiple linear regression analysis approach, proposed by Abraham et al. [45] has been used, which is represented by the following equation:

$$P = P^0 + a\alpha + b\beta + s\pi^*$$

where P is the value of the solvent dependent property to be modeled, P^0 , a , b and s are the coefficients determined from the regression analysis. The parameter π^* , is an index of the dielectric effects exerted by the solvent, α and β parameters [46] represent the hydrogen bond donating and accepting ability of the solvent, respectively. Correlations of $E(A)$ and $E(F)$, i.e. absorption and fluo-

rescence band maxima in cm^{-1} , respectively, were calculated against the above mentioned parameters. The following regression equations were obtained for 9-MA with good correlation factors (0.986 and 0.997 for $E(A)$ and $E(F)$ respectively);

$$E(A) = 27544 + 57.1\alpha + 100.5\beta - 59.5\pi^*$$

$$E(F) = 22779 - 831.1\alpha - 180.9\beta - 814.3\pi^*$$

The ratio of the regression coefficients of the parameters α and β denotes the relative importance of hydrogen bond donation over acceptance by the solvents towards the fluorophore [37,45]. The ratio is 0.57 in case of $E(A)$, indicating relatively weak hydrogen bonding interaction in the ground state, whereas for $E(F)$, the ratio is ~4.6, indicating that the ability of the solvent to act as a hydrogen bond donor plays a crucial role in the excited state. On the other hand, the high value of the regression coefficient corresponding to the solvent dielectric function (π^*) in the excited state also reveals a substantial effect of solvent polarity on the excited fluorophore, which is quite likely owing to the enhanced dipole moment of the emissive state.

Fluorescence lifetime study

Representative time-resolved decay profiles and corresponding residuals of 9-MA in different solvents are displayed in Fig. 4 and

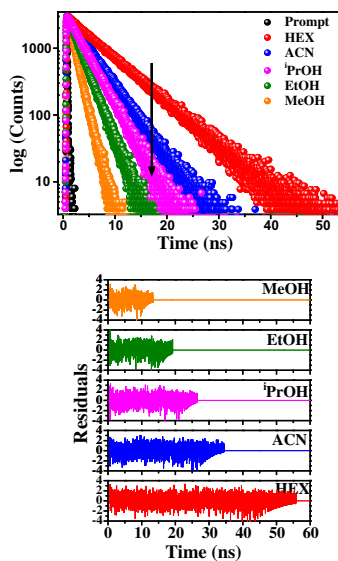


Fig. 4. Typical fluorescence decay profiles of 9-methyl anthroate associated with the lamp profile in different solvents and the plot of residuals corresponding to the fluorescence decays (top and bottom respectively); $\lambda_{\text{exc}} = 375 \text{ nm}$.

Table 2

Fluorescence decay parameters along with radiative and non-radiative rate constants of 9-methyl anthroate in various solvents.

Solvents	$E_T(30)$	Lifetime (ns)	χ^2	$k_r (\times 10^7)/\text{s}^{-1}$	$k_{nr} (\times 10^7)/\text{s}^{-1}$
HEX	30.9	9.27	1.04	2.170	8.616
CY	31.2	9.29	1.12	2.084	8.674
CCl ₄	32.5	9.01	1.06	2.789	8.308
THF	37.4	8.83	1.10	2.326	8.997
DCM	41.1	8.66	1.09	3.509	8.039
DMF	43.8	8.26	1.09	1.467	10.629
DMSO	45.0	8.18	1.03	1.627	10.587
ACN	46.0	5.26	1.03	2.024	16.971
iPrOH	48.6	4.11	1.04	1.410	22.890
BuOH	50.2	4.43	1.05	1.700	20.845
EtOH	51.9	2.89	1.04	1.518	32.982
MeOH	55.5	1.72	1.05	1.270	56.822

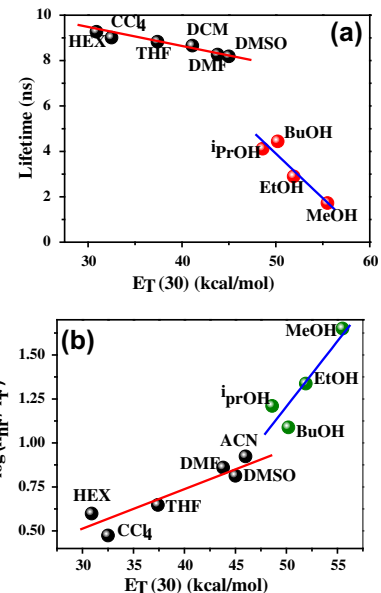


Fig. 5. (a) Plot of fluorescence lifetime (ns) vs. polarity parameter ($E_T(30)/\text{kcal mol}^{-1}$) for 9-methyl anthroate, as obtained in various solvents. (b) Variation of $\log(k_{nr}/k_r)$ as a function of polarity parameter ($E_T(30)/\text{kcal mol}^{-1}$) of solvents.

the relevant data are summarized in Table 2. The compound is found to exhibit a single-exponential decay pattern in all the assayed solvents except water where a bi-exponential decay is observed. From the correlation between lifetime of the excited state and solvent dependent $E_T(30)$ parameter (Fig. 5a), it's evident that the lifetime of the emissive state changes very little from non-polar to polar aprotic solvents, but a significant change is observed in polar protic solvents. For instance, the lifetime of the compound in polar protic isopropanol (~4.12 ns) is found to be much lower than the corresponding lifetime in polar aprotic DMSO (~8.18 ns) which in turn closely resembles the lifetime in non-polar *n*-hexane (~9.27 ns). Again, the steep change of lifetime from isopropanol to methanol (~1.72 ns) is noteworthy. Such observations can be explained on the basis of opening of parallel non-radiative channels operative in polar protic solvents via formation of intermolecular hydrogen-bonding between the ester and the solvent which leads to depletion of the fluorescence lifetime [38,43]. In case of water, the average lifetime (τ_{av}) is found to be ~1 ns, which is the average of a lower amplitude component with a lifetime of 6.04 ns ($\alpha = 0.032$) and another faster component (360 ps) with a higher amplitude ($\alpha = 0.971$). Considering the trend of depletion of lifetime of this compound with increasing H-bonding ability of the solvents, the faster component can be unambiguously assigned to the free ester (structure without any imposed rigidity) in water, whereas the other component with a considerably longer lifetime may arise from rigid intermolecular H-bonded cluster of the ester, which is possibly formed in the excited state by virtue of small size and excellent efficiency of H-bond formation of water [35]. This type of cluster formation may induce an added degree of rigidity to the entire molecular architecture and thereby reducing the vibrational degrees of freedom, a direct consequence of which may be the enhancement of fluorescence lifetime [37].

To rationalize the effect of solvents on the dynamics of the excited state, the radiative [$k_r = \Phi_f/\tau_f$] and non-radiative [$k_{nr} = (1 - \Phi_f)/\tau_f$] rate constants were calculated using fluorescence quantum yields (Φ_f) and lifetimes (τ_f) of the compound in different solvents. The values of k_r and k_{nr} in different solvents are presented in Table 2. The non-radiative rate constant values for 9-MA show significant sensitivity towards solvent polarity. The variation of $\log(k_{nr}/k_r)$ with $E_T(30)$ has been depicted in Fig. 5b. From a close

scrutiny of the figure, it is observed that with increasing solvent polarity, the $\log(k_{nr}/k_r)$ value of the compound increases gradually and shows a steep rise in case of polar protic solvents, which in turn strengthens our proposition of opening of deactivating non-radiative channels in protic solvents owing to solute–solvent hydrogen bonding.

Urea induced hydrogen bonding disruption study

Urea has long been known as a reagent which can efficiently perturb hydrogen bonding [47,48]. Though the exact mechanism is still a matter of debate, till date two mechanisms have been popular to explain such observations. One is an indirect mechanism in which urea is believed to act only at the level of the solvent, altering the structure of water in a way that facilitates dissolution of hydrophobic probes, i.e. by invoking the capacity of urea as “water structure breaker” [49].

The description on the classical hydrophobic effect given by Sinanoglu [50], states that when a nonpolar solute is dissolved in aqueous media, the dissolution process starts with the formation of a “cavity” in the solvent network in order to accommodate the solute. Breslow [51,52] in his work documented that the presence of urea results in an increase of the energetic cost associated with the cavity formation. Hence the direct mechanism of action of urea came into operation in which urea was proposed to participate in the solvation of the hydrophobic species by replacing some water molecules from the hydration shell of the solute. Thus an intrinsic interaction between the chaotrope and the hydrophobic substrate must exist to overcome the enhanced thermodynamic difficulties associated with the cavity formation. Herein, we have designed our experiment in a manner so as to delve into the effect of addition of urea on the hydrogen bonded probe in aqueous medium. For this purpose, the absorption and emission spectral properties of the probe has been monitored with increasing urea concentration in aqueous medium. Furthermore, with a view to establish the impact of externally added chaotrope on the H-bonded probe, time resolved emission study has also been done.

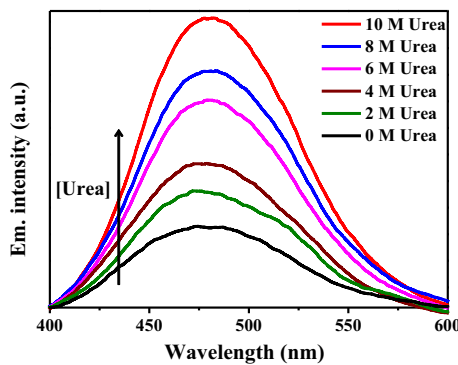


Fig. 6. Fluorescence emission spectra of 9-methyl anthroate in aqueous medium in presence of various concentrations of urea as indicated in the figure legend. (Exciting at the corresponding absorption band maximum).

Table 3

Quantum yield values and fluorescence decay parameters of 9-methyl anthroate in aqueous medium having various concentrations of urea.

(Urea) in M	Quantum yield (Φ)	α_1	α_2	τ_1 (ns)	τ_2 (ns)	τ_{av} (ns)	χ^2
0	0.010	0.970	0.032	0.360	6.04	2.384	1.03
4	0.017	0.984	0.016	0.402	4.94	1.160	1.07
8	0.028	0.988	0.012	0.573	3.72	0.805	1.08
10	0.035	0.958	0.043	0.628	1.39	0.698	0.99

The presence of urea is, however, found to induce no significant modification to the qualitative appearance of the absorption profile compared to that in the absence of the same (Figure not shown). The impact of added urea is more conspicuously seen through quantitative perusal of the emission intensity as shown in Fig. 6, where a substantial increase in intensity as well as in quantum yield is observed, without any observable spectral shift. The corresponding quantum yield values are presented in Table 3. The increasing value of quantum yield of the ester with increasing concentration of urea advocates for the decrement of non radiative decays owing to urea induced disruption of H-bonds.

By virtue of its sensitivity to the associated environment of a probe, fluorescence lifetime serves as an indicator to explore the microenvironment around a fluorophore [28,47]. Fig. 7 illustrates the typical time-resolved fluorescence decay profiles of the probe in aqueous medium in presence of various amounts of urea as indicated in the figure legends and the corresponding fitting parameters are collected in Table 3. As stated earlier, 9-MA shows a bi-exponential decay in aqueous medium, a lower amplitude component with a lifetime of ~ 6 ns ($\alpha = 0.032$) and another faster component (360 ps) with a higher amplitude ($\alpha = 0.971$), and we assigned the faster component to the free ester in water, whereas the other component was assumed to be arising from the rigid intermolecular H-bonded cluster of the ester. Interestingly, with the addition of urea the lifetime assigned to the rigid cluster significantly reduces whereas the other corresponding to the free probe does not substantially alter (although an increment is observed, which might be due to the depletion of non radiative decay rates in presence of urea) and the individual contributions of both the species remain almost constant and thus a depletion of the average lifetime of the ester is observed. The above mentioned observation can be rationalized considering the efficacy of urea to participate in the solvation of the hydrophobic species by replacing some water molecules from the hydration shell of the solute and thereby promoting the rupture of the formed H-bonded cluster, which results in a decrement of the corresponding lifetime due to negation of the imposed rigidity.

Analysis of quantum chemical calculations

The ground state global minimum geometry of 9-MA in vacuo at DFT level (B3LYP/6-311++G(d,p)) shows that the ester group is twisted and out of plane of the anthryl ring by $\sim 56^\circ$ (Scheme 1, angle represented by θ). As mentioned earlier, the calculated dipole moment for the ground state structure is found to be 1.76 D at the same level of theory. The pictures of the HOMO and LUMO of the compound in the ground state are shown in Fig. 8, which reveal a more or less uniform distribution of the π cloud density over the entire system for the optimized structure of the ester for both the molecular orbitals. This is a corroboration of the presence of an extensive delocalization in the ground state through the entire π network of the system and predicts the $\pi-\pi^*$ (allowed) nature of the transition, also further supported by high oscillator strength value of 0.2556, obtained by TDDFT method using the same basis set. TDDFT calculation also predicts the first vertical transition $S_1 \leftarrow S_0$ of the ester in vacuo, at wavelength 335.77 nm which is in good agreement with the experimental values obtained via absorption spectroscopy. To gather information about the effect of solvent polarity on the compound in the ground state, the structure has been optimized in presence of solvent using the PCM (Polarizable Continuum Model) method and the results are summarized in Table S1 of the Supporting information. As expected, in the ground state with increasing polarity of the solvent there is an increase in dipole moment which leads to stabilization in polar media and an increase in the twisting angle (θ) is also observed

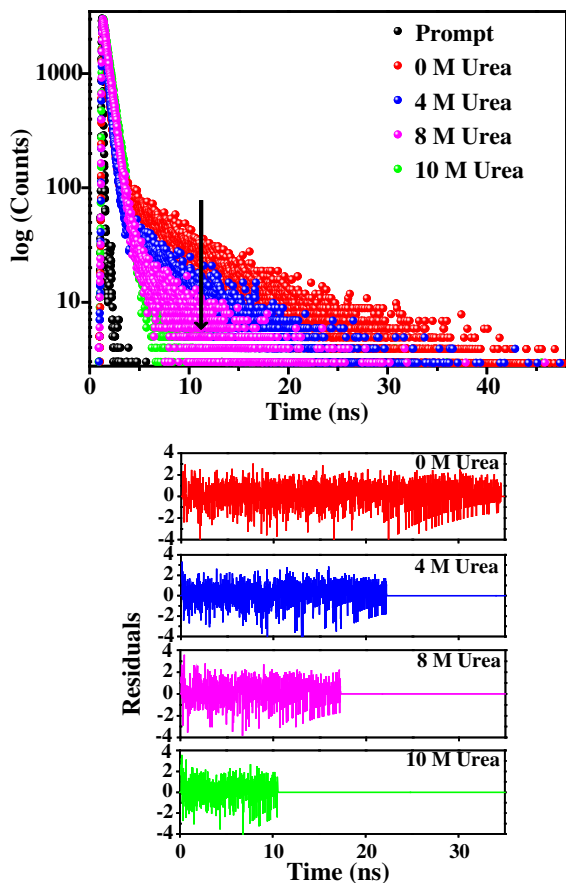


Fig. 7. Typical fluorescence decay profiles of 9-methyl anthroate associated with the lamp profile in aqueous medium differing in urea concentrations and the plot of residuals corresponding to the fluorescence decays (top and bottom respectively); $\lambda_{\text{exc}} = 375 \text{ nm}$.

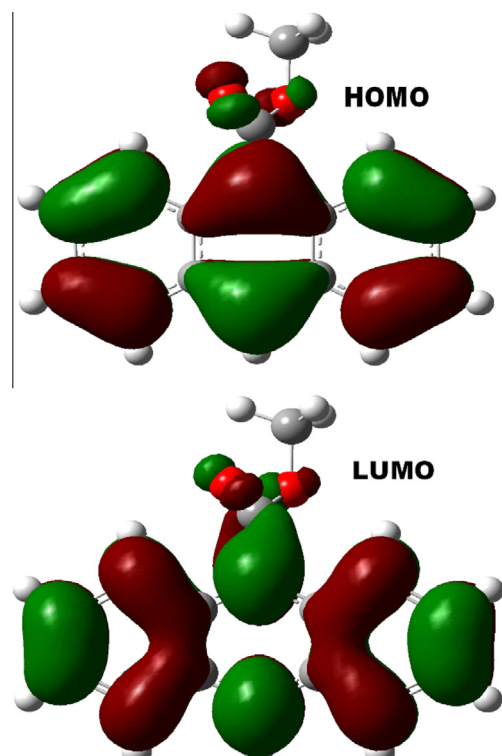


Fig. 8. HOMO and LUMO diagram generated from the optimized structure of the ester at DFT level (B3LYP/6-311++G(d,p)).

which might be argued to be the reason behind the observed enhancement in dipole moment.

The excited state global minimum geometry of 9-MA in vacuo obtained at TD-DFT level of theory (using the same basis set) shows that here also the ester group is twisted and out of plane of the anthryl ring by $\sim 34^\circ$ (Table S1 in the Supporting information). The calculated dipole moment for the aforesaid structure is found to be 2.04 D at the same level of theory. The simulated emission spectra obtained from the optimized excited state predicts the emission maximum to be at $\sim 460 \text{ nm}$ having an oscillator strength of 0.0938, which fairly agrees with the experimental results.

Conclusion

The title compound 9-methyl anthroate (9-MA) was synthesized and its photophysical behavior has been studied spectroscopically as well as theoretically by means of quantum chemical calculations. Solvatochromic measurements predict the existence of a polar excited state. Higher dipole moment of the emissive FC state compared to the ground state is the sole reason for solvent polarity dependent red shifted emission band of the compound. On the other hand, the hydrogen-bonding interaction with the solvents is also responsible for the stability of the emissive state as is evident from the E_T (30) plots. Fluorescence quantum yields and lifetime data, along with the regression analysis also support the fact that in protic solvents, non-radiative decay of the emissive state is prominent owing to intermolecular hydrogen bonding interaction with the solvent. Theoretical studies also substantiate the presence of a Franck-Condon emissive state and accounts well for the polarity dependence of the emission spectra.

Acknowledgements

NG acknowledges Department of Science and Technology, India for financial assistance through Project No. SR/S1/PC-26/2008. AG gratefully acknowledges CSIR, New Delhi, India for Junior Research Fellowship. SJ, SG and SD would like to thank UGC for Research Fellowships.

Appendix A. Supplementary material

Supplementary data associated with this article can be found, in the online version, at <http://dx.doi.org/10.1016/j.saa.2013.04.059>.

References

- [1] H. Ihmels, A. Meiswinkel, C.J. Mohrschladt, Org. Lett. 2 (2000) 2865–2867.
- [2] C. Zimmermann, M. Mohr, H. Zippe, R. Eichberger, W. Schnabel, J. Photochem. Photobiol. A: Chem. 125 (1999) 47–56.
- [3] A. Debbab, A.H. Aly, R. Edrada-Ebel, V. Wray, A. Pretsch, G. Pescitelli, T. Kurtan, P. Proksch, Eur. J. Org. Chem. (2012) 1351–1359.
- [4] C. Huang, H. Jin, B. Song, X. Zhu, H. Zhao, J. Cai, et al., Appl. Microbiol. Biotechnol. 93 (2012) 777–785.
- [5] A.W. Wood, R.L. Chang, W. Levin, R.E. Lehr, M. Schaefer-Ridder, J.M. Karle, et al., Proc. Natl. Acad. Sci. USA 74 (1977) 2746–2750.
- [6] S. Bantia, A. Samanta, J. Phys. Chem. B 110 (2006) 6437–6440.
- [7] K. Ghosh, A.R. Sarkar, G. Masanta, Tetrahedron Lett. 48 (2007) 8725–8729.
- [8] S. Iwata, H. Matsuoka, K. Tanaka, J. Chem. Soc. Perkin Trans. 1 (1997) 1357–1360.
- [9] T. Gunnlaugsson, H.D.P. Ali, M. Glynn, P.E. Kruger, G.M. Hussey, F.M. Pfeffer, et al., J. Fluoresc. 15 (2005) 287–299.
- [10] Y. Wang, G. Qian, Z. Xiao, H. Wang, L. Long, H. Wang, et al., Inorg. Chim. Acta 363 (2010) 2325–2332.
- [11] P.I. Shih, C.Y. Chuang, C.H. Chien, E.W.G. Diau, C.F. Shu, Adv. Funct. Mater. 17 (2007) 3141–3146.
- [12] I.L. Lee, S.R. Li, K.F. Chen, P.J. Ku, A.S. Singh, H.T. Kuo, et al., Eur. J. Org. Chem. (2012) 2906–2915.
- [13] F. Wilkinson, D.J. McGarvey, A.F. Olea, J. Am. Chem. Soc. 115 (1993) 12144–12151.
- [14] D.A. Kelkar, A. Ghosh, A. Chattopadhyay, J. Fluoresc. 13 (2003) 459–466.

- [15] H. Bouas-Laurent, A. Castellan, J. Desvergne, R. Lapouyade, *Chem. Soc. Rev.* 29 (2000) 43–55.
- [16] I. Zouev, D. Cao, T.V. Sreevidya, M. Telzhensky, M. Botoshansky, M. Kaftory, *Cryst. Eng. Commun.* 13 (2011) 4376–4381.
- [17] T.C. Werner, W. Hawkins, J. Facci, R. Torrisi, T. Trembath, *J. Phys. Chem.* 82 (1978) 298–301.
- [18] I.I. Schuster, *J. Org. Chem.* 46 (1981) 5110–5118.
- [19] T.C. Werner, D.M. Hercules, *J. Phys. Chem.* 78 (1969) 2005–2011.
- [20] T.C. Werner, R.M. Hoffman, *J. Phys. Chem.* 77 (1973) 1611–1615.
- [21] J.R. Lakowicz, *Principles of Fluorescence Spectroscopy*, third ed., Springer, New York, 2006.
- [22] N.J. Turro, *Modern Molecular Photochemistry*, Benjamin/Cummings, Menlo Park, CA, 1978.
- [23] A. Chakraborty, S. Kar, N. Guchhait, *Chem. Phys.* 320 (2006) 75–83.
- [24] F.A.S. Chipem, A. Mishra, G. Krishnamoorthy, *Phys. Chem. Chem. Phys.* 14 (2012) 8775–8790.
- [25] E.C. Lim, *J. Phys. Chem.* 90 (1986) 6770–6777.
- [26] J.X. Kang, S.F.P. Man, N.E. Brown, P.A. Labrecque, M.T. Clandinin, *Biochem. J.* 285 (1992) 725–729.
- [27] R.C. Parish, L.I. Stock, *J. Org. Chem.* 30 (1965) 927–929.
- [28] B.K. Paul, N. Guchhait, *J. Phys. Chem. B* 115 (2011) 11938–11949.
- [29] B. Bhattacharya, S. Nakka, L. Guruprasad, A. Samanta, *J. Phys. Chem. B* 113 (2009) 2143–2150.
- [30] W. Rettig, B. Zietz, *Chem. Phys. Lett.* 317 (2000) 187–196.
- [31] S. Mahanta, R.B. Singh, S. Kar, N. Guchhait, *J. Photochem. Photobiol. A: Chem.* 194 (2008) 318–326.
- [32] M.J. Frisch, G.W. Trucks, H.B. Schlegel, G.E. Scuseria, M.A. Robb, J.R. Cheeseman, J.A. Montgomery Jr., T. Vreven, K.N. Kudin, J.C. Burant, J.M. Millam, S.S. Iyengar, J. Tomasi, V. Barone, B. Mennucci, M. Cossi, G. Scalmani, N. Rega, G.A. Petersson, H. Nakatsuji, M. Hada, M. Ehara, K. Toyota, R. Fukuda, J. Hasegawa, M. Ishida, T. Nakajima, Y. Honda, O. Kitao, H. Nakai, M. Klene, X. Li, J.E. Knox, H.P. Hratchian, J.B. Cross, C. Adamo, J. Jaramillo, R. Gomperts, R.E. Stratmann, O. Yazyev, A.J. Austin, R. Cammi, C. Pomelli, J.W. Ochterski, R.L. Martin, K. Morokuma, V.G. Zakrzewski, G.A. Voth, P. Salvador, J.J. Dannenberg, S. Dapprich, A.D. Daniels, O. Farkas, J.B. Foresman, J.V. Ortiz, J. Cioslowski, D.J. Fox, Gaussian 09, Revision A.02-SMP, Gaussian, Inc., Wallingford, CT, 2009.
- [33] M.J. Frisch, G.W. Trucks, H.B. Schlegel, G.E. Scuseria, M.A. Robb, J.R. Cheeseman, G. Scalmani, V. Barone, B. Mennucci, G.A. Petersson, H. Nakatsuji, M. Caricato, X. Li, H.P. Hratchian, J.B. Cross, C. Adamo, J. Jaramillo, R. Gomperts, R.E. Stratmann, O. Yazyev, A.J. Austin, R. Cammi, C. Pomelli, J.W. Ochterski, R.L. Martin, K. Morokuma, V.G. Zakrzewski, G.A. Voth, P. Salvador, J.J. Dannenberg, S. Dapprich, A.D. Daniels, O. Farkas, J.B. Foresman, J.V. Ortiz, J. Cioslowski, D.J. Fox, Gaussian 09, Revision A.02-SMP, Gaussian, Inc., Wallingford, CT, 2009.
- [34] W.J. Hehre, L. Radom, P.V. Schleyer, J.A. Pople, *Ab Initio Molecular Orbital Theory*, Wiley, New York, 1986.
- [35] B.K. Paul, S. Mahanta, R.B. Singh, N. Guchhait, *J. Phys. Chem. A* 114 (2010) 2618–2627.
- [36] E. Lippert, W. Luder, H. Boos, in: A. Mangini (Ed.), *Advances in Molecular Spectroscopy*, 443, Pergamon Press, Oxford, 1962.
- [37] B.K. Paul, A. Samanta, S. Kar, N. Guchhait, *J. Lumin.* 130 (2010) 1258–1267.
- [38] S. Dhar, D.K. Rana, S.S. Roy, S. Roy, S. Bhattacharya, S.C. Bhattacharya, *J. Lumin.* 132 (2012) 957–964.
- [39] G. Köhler, K. Rechthaler, *Pure Appl. Chem.* 65 (1993) 1647–1652.
- [40] S. Jana, S. Dalapati, S. Ghosh, S. Kar, N. Guchhait, *J. Mol. Struct.* 998 (2011) 136–143.
- [41] S. Ghosh, A. Chakraborty, S. Kar, N. Guchhait, *Spectrochim. Acta A* 75 (2010) 320–324.
- [42] C. Reichardt, *Chem. Rev.* 94 (1994) 2319–2358.
- [43] A. Sarkar, T.K. Mandal, D.K. Rana, S. Dhar, S. Chall, S.C. Bhattacharya, *J. Lumin.* 130 (2010) 2271–2276.
- [44] A. Mishra, G. Krishnamoorthy, *Photochem. Photobiol. Sci.* 11 (2012) 1356–1367.
- [45] M.H. Abraham, P.L. Greillier, J.L.M. Abboud, R.M. Doherty, R.W. Taft, *Can. J. Chem.* 66 (1988) 2673–2686.
- [46] M.J. Kamlet, J.L.M. Abboud, M.H. Abraham, R.W. Taft, *J. Org. Chem.* 48 (1983) 2877–2887.
- [47] B.K. Paul, N. Guchhait, *J. Colloid Interf. Sci.* 353 (2011) 237–247.
- [48] A.K. Soper, E.W. Castner, A. Luzar, *Biophys. Chem.* 105 (2003) 649–666.
- [49] N. Müller, in: E.A. Cordes (Ed.), *Reaction Kinetics in Micelles*, Plenum, New York, 1973.
- [50] O. Sinanoglu, in: B. Pullman (Ed.), *Molecular Associations in Biology*, Academic Press, New York, 1968.
- [51] R. Breslow, T. Guo, *Proc. Natl. Acad. Sci. USA* 87 (1990) 167–169.
- [52] R. Breslow, *Acc. Chem. Res.* 24 (1991) 159–164.